

## Comparison of Transient Electron Heat Transport in LHD Helical and JT-60U Tokamak Plasmas

S. Inagaki<sup>1</sup>, H. Takenaga<sup>2</sup>, K. Ida<sup>1</sup>, A. Isayama<sup>2</sup>, N. Tamura<sup>1</sup>, T. Takizuka<sup>2</sup>, T. Shimosuma<sup>1</sup>, Y. Kamada<sup>2</sup>, S. Kubo<sup>1</sup>, Y. Miura<sup>2</sup>, Y. Nagayama<sup>1</sup>, K. Kawahata<sup>1</sup>, S. Sudo<sup>1</sup>, K. Ohkubo<sup>1</sup>,  
LHD Experimental Group and the JT-60U Team

- 1) National Institute for Fusion Science, Oroshi-cho, Toki-shi, Gifu, 509-5292, Japan
- 2) Naka Fusion Research Establishment, Japan Atomic Energy Research Institute, Naka-machi, Naka-gun, Ibaraki 311-0193, Japan

e-mail contact of main author : inagaki@LHD.nifs.ac.jp

**Abstract.** Transient transport experiments are performed in plasmas with and without Internal Transport Barrier (ITB) on LHD and JT-60U. The dependence of  $\chi_e$  on electron temperature,  $T_e$ , and electron temperature gradient,  $\nabla T_e$ , is analyzed by an empirical non-linear heat transport model. In plasmas without ITB, two different types of non-linearity of the electron heat transport are observed from cold/heat pulse propagation. The  $\chi_e$  depends on  $T_e$  in LHD, while it depends not only on  $T_e$  but also on  $\nabla T_e$  in JT-60U. In ITB plasmas, a cold pulse growing driven by the negative  $T_e$  dependence of  $\chi_e$  is commonly observed both in LHD and JT-60U.

### 1. Introduction

Helical systems and tokamaks are the most realistic concepts for magnetic confinement of thermonuclear plasmas. There are some similarities and differences in heat transport between helical systems and tokamaks. Similarities in transport are as following: (i) the radial heat transport is anomalously higher than neoclassical theory, (ii) the global energy confinement time shows similar parametric dependence and the power degradation of confinement is observed in both devices. Heat (and particle) transport in both devices are also considered to be driven by turbulent processes. On the other hand, one of the differences in heat transport is as following: the  $T_e$  profile reacts weakly to changes of the heating deposition profile in tokamaks, however, this transport phenomenon, known as “profile stiffness” [1, 2], is weak or absent in helical systems. In fact, although the global confinement scaling is similar to ELMy H-mode scaling [3], no evidence for the tokamak-like stiffness is observed in the Large Helical Device (LHD). The physical models that can explain stiffness can be divided into two categories: local and non-local. Some local transport models based on temperature-gradient-driven turbulence indicate that the heat transport is non-linear and thus the electron heat diffusivity,  $\chi_e$ , has a dependence on  $T_e$ , and/or  $\nabla T_e$  [4, 5]. Especially, the non-linear models based on the “critical gradient scale length” can explain some of tokamak-type stiffness [6]. However the “critical gradient scale length” is unclear in the LHD inward shifted configuration (major radius at the magnetic axis,  $R_{ax} = 3.5\text{m}$ , an averaged plasma radius,  $a_p = 0.58$ ). Figure 1 shows the  $T_e$  and temperature scale length,  $L_T^{-1} = -\nabla T_e/T_e$ , dependence of  $\chi_e$  in the LHD NBI plasma (neutral beam heating power,  $P_{NB} \sim 2\text{-}6\text{MW}$ , line averaged density,  $\bar{n}_e = 1\text{-}3 \times 10^{19}\text{m}^{-3}$ ). Although the  $T_e$  dependence of  $\chi_e$  is clear,  $L_T^{-1}$  dependence of  $\chi_e$  is unclear in the power balance analysis. Therefore, the validity of non-linear transport models based on turbulence should be clarified in helical systems to establish first-principle transport models. To study the non-linearity of heat transport, transient transport analysis is recognized as a very powerful tool because it can yield  $\partial q_e/\partial \nabla T_e$  and  $\partial q_e/\partial T_e$  [7]. In addition, the transient analysis is the only technique which can obtain information to answer the interesting question of whether transport in magnetically confined plasmas

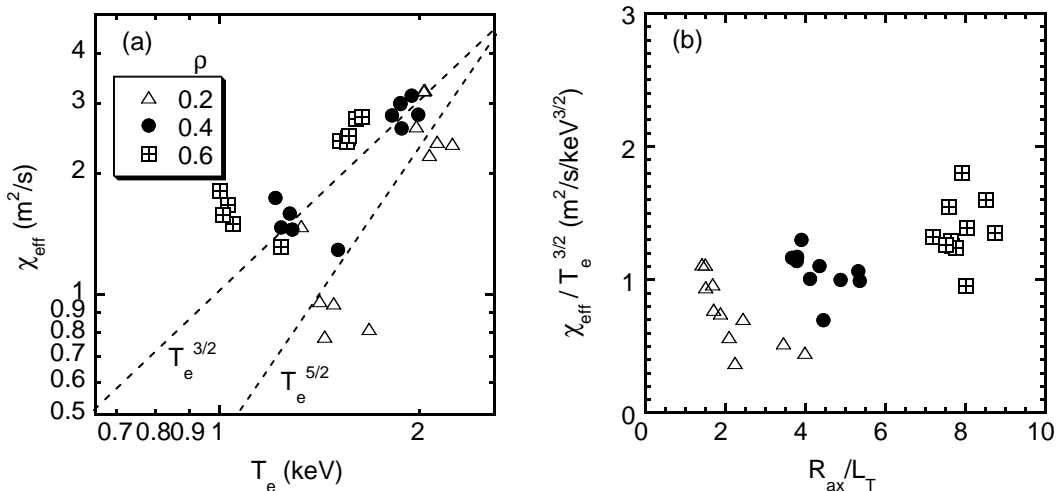


FIG. 1: (a)  $T_e$  and (b)  $L_T$  dependence of  $\chi_e$  at different radii in the LHD NBI plasmas. The  $\chi_e$  is normalized by the gyro-Bohm  $T_e$  dependence in (b)

is determined by local plasma parameters or not.

Theoretically, the magnetic configuration influences turbulence in many aspects. Hence, comparison of heat transport features between tokamak and helical systems would reveal the importance of the magnetic configuration for transport and be very useful to gain a comprehensive understanding of the turbulent transport in toroidal devices because their magnetic configurations are quite different (e.g. aspect ratio and safety factor,  $q$ , profile). Recent experimental progress on LHD and JT-60U enables us to make more an extensive comparison of the transient response in plasmas not only without ITB but also with ITB. In this paper, the newly obtained results of transient transport experiments are reported and the characteristics of electron transport obtained from transient analysis are compared between LHD and JT-60U plasmas.

## 2. Transient transport experiments

In order to induce a cold pulse, a tracer encapsulated solid pellet (TESPEL [8]) is injected into the LHD edge. Figure 2(a) shows the typical time evolution of cold pulse induced by TESPEL injection in the low power NBI plasma on LHD (neutral beam injection power  $P_{NB} \sim 3$  MW, line averaged density  $\bar{n}_e = 2 \times 10^{19} \text{m}^{-3}$ ). To study the non-linearity between heat flux and temperature gradient in toroidal plasma, the transient transport analysis is carried out with a simple non-linear model for  $\chi_e$  written as  $\chi_e \propto T_e^\alpha |\nabla T_e|^\beta$ . By using this model, the perturbed electron heat transport equation can be written as,

$$\frac{3}{2} n_e \frac{\partial \delta T_e}{\partial t} = \nabla \cdot \left( n_e (1 + \beta) \chi_e \nabla \delta T_e - n_e \alpha \chi_e \frac{\delta T_e}{L_T} \right). \quad (1)$$

Here  $n_e$ ,  $\nabla T_e$ ,  $T_e$  and  $\chi_e$  are static values obtained just before TESPEL injection,  $\delta T_e = T_{e,t=0} - T_e(r, t)$  and  $\chi_e$  can be estimated by the static analysis i.e. power balance analysis. The  $n_e$  increases in the ablation region ( $\rho > 0.6$ ) while it doesn't change in core region within the accuracy of the Abel inversion. The particle diffusivity, which is estimated by gas-puff modulation experiments [9] is much smaller than  $\chi_e$  and thus the particle transport effects on the cold pulse propagation are neglected in the LHD. When the heat flux perturbation,  $\delta q_e(r, t)$ , and the

perturbation scale length,  $L_{\delta T_e}$ , are defined as

$$\delta q_e(r, t) = \frac{1}{r} \int_0^r \frac{3}{2} n_e \frac{\partial \delta T_e}{\partial t} \rho d\rho, \quad L_{\delta T_e}(r, t) = (\nabla \delta T_e / \delta T_e)^{-1},$$

Eq. 1 can be written as

$$\frac{\delta q_e}{n_e \delta T_e} = \frac{\chi_{tr}}{L_{\delta T_e}} - V_{tr}, \quad (2)$$

here  $\chi_{tr} = (1 + \beta)\chi_e$ ,  $V_{tr} = \alpha\chi_e L_T^{-1}$  and  $r$  is the averaged minor radius. Figure 2(b) shows the time trace of plasma in the gradient - flux space for a cold pulse propagation. The fact that data points indeed lay on a straight line allows us to determine  $\beta$  and  $\alpha$  from the slope and intercept of a line. The obtained  $\chi_{tr}$  is shown in Fig. 2(c). The heat diffusivity estimated by power balance analysis,  $\chi_{pb}$ , is also shown. The small difference between  $\chi_{pb}$  and  $\chi_{tr}$  indicates a weak  $\nabla T_e$  dependence of  $\chi_e$  ( $\beta \ll 1$ ) in LHD. On the contrary, the  $T_e$  dependence of  $\chi_e$  is indicated in Fig. 2(d). A gyro-Bohm like  $T_e$  dependence ( $\alpha = 3/2 - 5/2$ ) can explain the obtained  $\alpha$ . Although the  $\alpha$  in the edge region is more important to compare with the global energy confinement and it has not obtained by transient analysis,  $T_e$  dependence of  $\chi_e$  can be considered as one of the candidates to explain the power degradation of the global confinement in LHD [3]. In high NB power cases, however, the non-local  $T_e$  rise, which is discussed later, appears and it makes hard to decouple the non-linearity of  $\chi_e$  from observations.

To perturb the core region of JT-60U H-mode plasma, the short pulse (100ms) ECH injection is carried out. Figure 3(a) shows the typical response of  $T_e$  to a step of the injected ECH power ( $P_{EC} \sim 1\text{MW}$ ) in the core region. Here, the peak of ECH power deposition is located at  $\rho \sim 0.6$ , and there is no ECH power source in the region of  $\rho < 0.3$ . The heat pulse propagates from edge to core similar to the cold pulse and thus the transient analysis with an empirical non-linear  $\chi_e$  model, which is discussed above, can be applied (see Fig. 3(b)). The  $\chi_{tr} = 0.16\text{m}^2/\text{s}$  is obtained in an ohmic plasma while the  $\chi_{tr}$  increases in the NBI plasma ( $0.24\text{m}^2/\text{s}$ ) due to the increase in  $T_e$  or  $\nabla T_e$ . To compare the  $\nabla T_e$  dependence of  $\chi_e$  with the critical gradient length model, both  $\chi_{tr}$  and  $\chi_{pb}$  are plotted as a function of  $R_{ax}/L_T$  (see Fig. 3(c)). The  $\chi_{pb}$  and the  $\chi_{tr}$  are normalized by  $T_e^{3/2}$  to decouple the gyro-Bohm  $T_e$  dependence. The dependence of  $\chi_{pb}$  on  $R_{ax}/L_T$  may be changed at  $R_{ax}/L_T = 6 - 8$  i.e. the temperature-gradient-driven mode may be switched on above  $R_{ax}/L_T = 6-8$  and  $\chi_e$  has  $\nabla T_e$  dependence, and thus the enhancement of  $\chi_{tr}$  ( $\chi_{tr} > \chi_{pb}$ ) may be observed at  $R_{ax}/L_T = 6-8$ . The  $\nabla T_e$  dependence factor  $\beta$  decreases from 3 to 1.6 with the increase in  $R_{ax}/L_T$ , while the  $\nabla T_e$  dependence factor  $\alpha = 0.5 - 2$  is not different from that obtained in the LHD plasma.

There are differences in non-linearity of  $\chi_e$  between LHD and JT-60U plasmas without ITBs. The  $T_e$  dependence of  $\chi_e$  is larger than  $\nabla T_e$  dependence in LHD plasma. On the other hand, a  $\nabla T_e$  dependence of  $\chi_e$  is observed in JT-60U plasma. For the stabilization of micro-turbulence, the local shear is a critical parameter [10]. The influence of local and global shear on turbulence may be one of the candidates to explain the difference in the non-linearity between LHD and JT-60U plasmas.

### 3. Cold pulse propagations in plasmas with electron internal transport barrier

The transport barriers are considered to be formed by the suppression of turbulence-induced transport both in helical systems and tokamaks, however some important questions, such as whether the transport in the ITB is diffusive or convective and whether it is still stiff or not, have

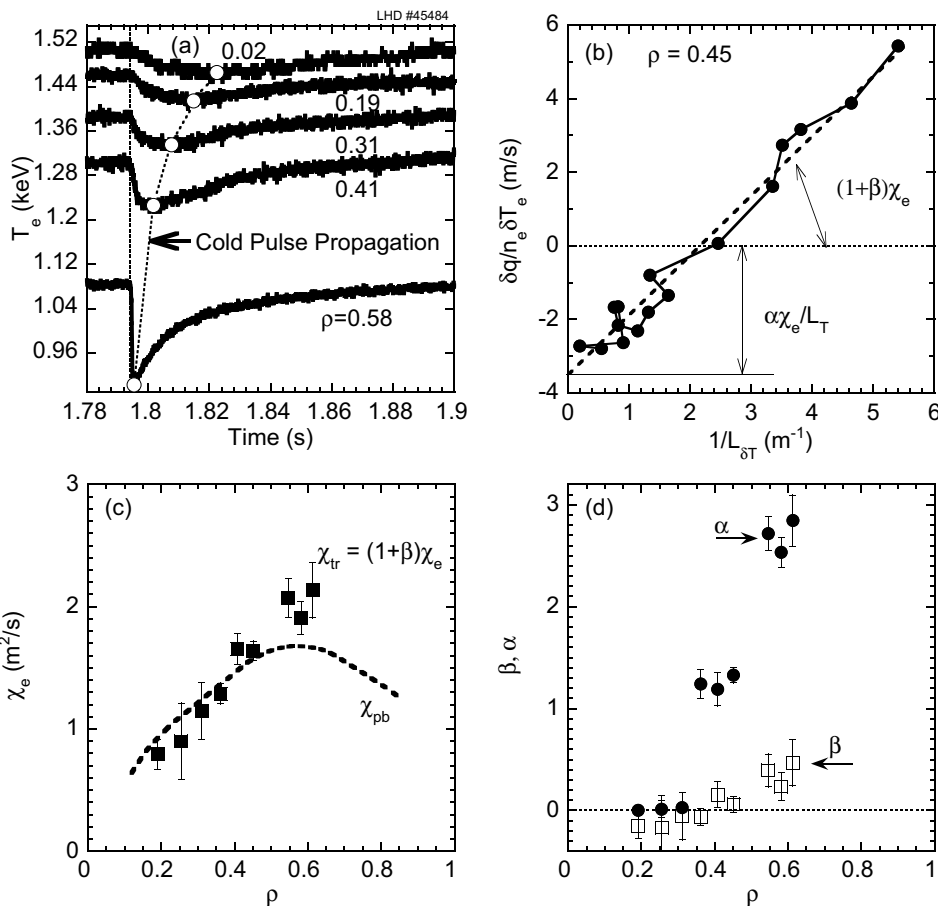


FIG. 2: (a) time evolution of  $T_e$  perturbations induced by TESPEL injection at different radii, (b) behavior of plasma at  $\rho = 0.45$  in the perturbed gradient vs the perturbed heat flux space, (c) radial profiles of  $\chi_{tr}$  and  $\chi_{pb}$ , (d) radial profiles of  $\beta$  (the index of  $\nabla T_e$  dependence of  $\chi_e$ ) and  $\alpha$  (the index of  $T_e$  dependence of  $\chi_e$ )

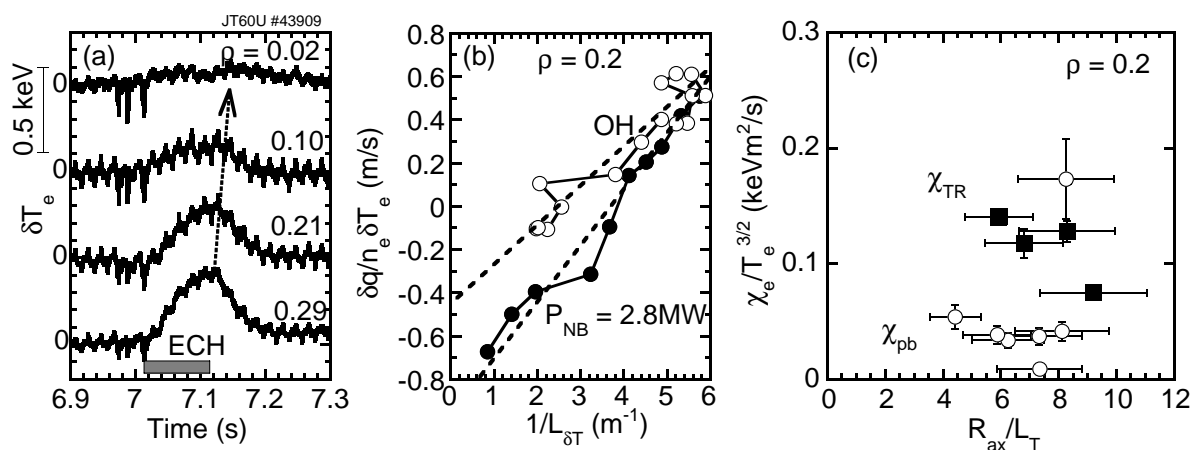


FIG. 3: (a) Time evolution of  $T_e$  perturbations induced by a step of the ECH in JT-60U ( $\rho < 0.3$ ), (b) typical behavior of ohmic and NBI plasmas in the perturbed gradient and the perturbed heat flux space ( $I_p = 0.8MA$ ), (c)  $R_{ax}/L_T$  dependence of  $\chi_{pb}$  and  $\chi_{tr}$ , here the  $\chi_{pb}$  and the  $\chi_{tr}$  are obtained in the density region of  $n_{e0} = 1.6 - 2.5 \times 10^{19} m^{-3}$

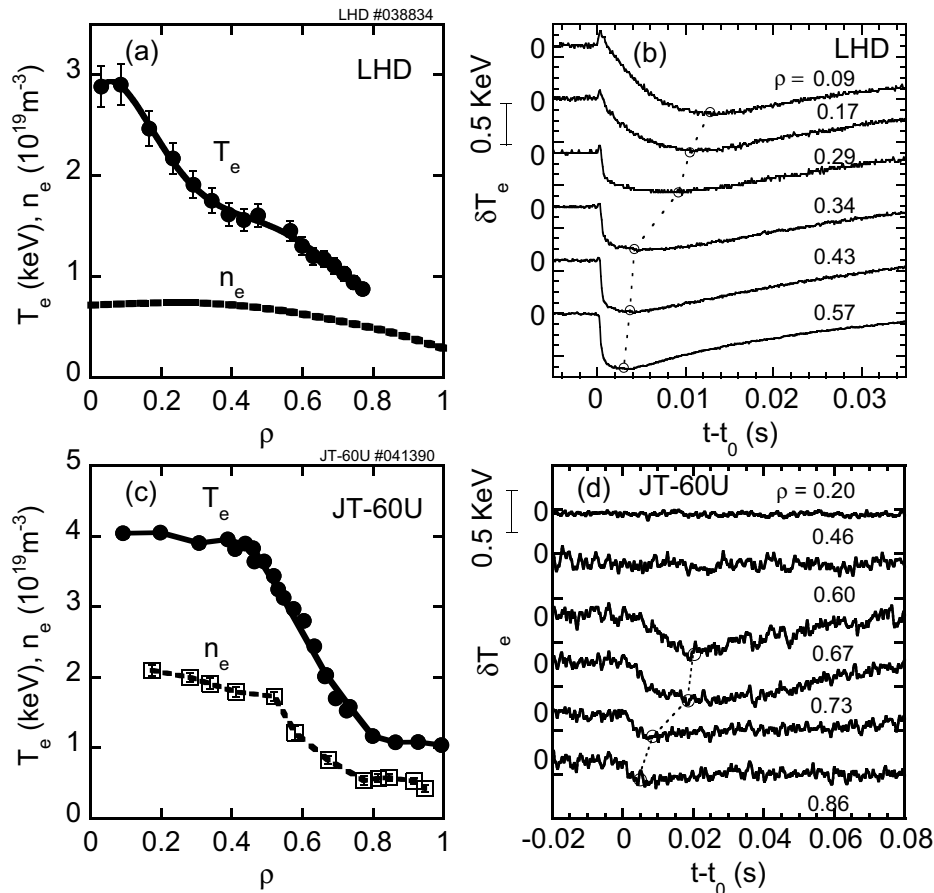


FIG. 4: Radial profiles of  $e$ -ITB plasmas just before TESPEL/Pellet injection in (a) LHD and (c) JT-60U, and time response of  $T_e$  to edge cooling in (b) LHD and (d) JT-60U. The TESPEL/Pellet is injected at  $t = t_0$ .

not been answered yet. Transient experiments are relevant for these issues to be clarified.

The  $e$ -ITB is formed when the ECH is focused on the magnetic axis in LHD ( $P_{EC} \sim 0.8 \text{MW}$ ,  $P_{NB} \sim 2 \text{MW}$ ,  $R_{ax} = 3.5 \text{m}$ ,  $a_p = 0.58 \text{m}$ ,  $\bar{n}_e = 0.7 \times 10^{19} \text{m}^{-3}$ ), and it is formed in the reversed shear plasma [11] on JT-60U ( $P_{NB} = 7.6 \text{MW}$ ,  $R_{ax} = 3.4 \text{m}$ ,  $a_p = 0.94 \text{m}$ ,  $\bar{n}_e = 1.5 \times 10^{19} \text{m}^{-3}$ ,  $I_p = 1 \text{MA}$ ). Typical time evolutions of cold pulse propagation and radial profiles of target plasmas are shown in Fig. 4. There is also an ion barrier ( $T_{i0} = 7 \text{keV}$ ) in the JT-60U plasma, while neither ion nor  $n_e$  ITBs are present in LHD ( $T_{i0} = 1.8 \text{keV}$ ). The cold pulse propagation technique is also used to perturb the ITB plasmas. The TESPEL (in LHD) and the pellet (in JT-60U) are injected to the edge of  $e$ -ITB plasmas. A unique feature of cold pulse propagation is observed. When the cold pulse approaches the ITB foot, the negative peak of the cold pulse is enhanced both in JT-60U and LHD as shown in Fig. 5 (a) and (b). Here, no evidence of a significant plasma shift induced by the TESPEL/PELLET injection is observed. In the JT-60U plasma, the cold pulse is damped strongly to zero further inside the ITB region, and thus there is no perturbation in the core. The cold pulse reaches to the core in LHD plasma, however, the slowing down of the cold pulse propagation inside the ITB is observed as shown in Fig. 4(b). In addition, the temperature returns to the previous profile in spite of the increase in density after TESPEL/PELLET injection. Thus these enhancements of the cold pulse cannot be due to the backforward transition of the ITB. The simple diffusive nature (heat flux is proportional

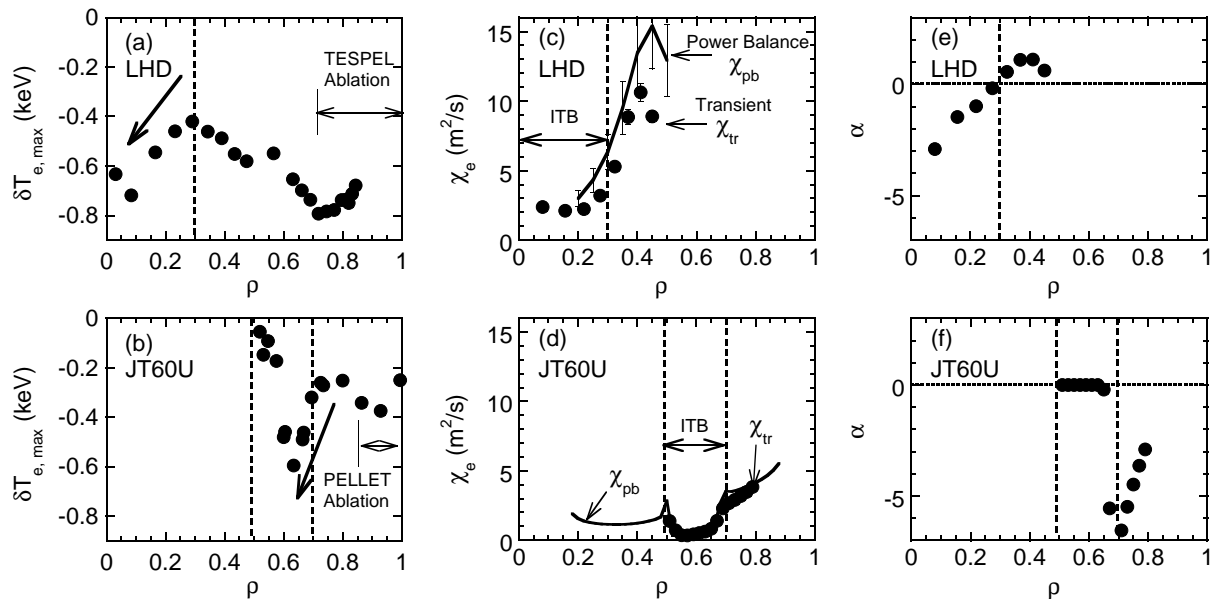


FIG. 5: Radial profiles of the cold pulse peak in (a) LHD and (b) JT-60U, the transient and powerbalance heat diffusivity in (c) LHD and (d) JT-60U and the  $T_e$  dependence factor of  $\chi_e$  in (e) LHD and (d) JT-60U.

to temperature gradient) cannot explain this enhancement of the cold pulse. The non-linear dependence of  $\chi_{tr}$  on  $T_e$  and/or  $\nabla T_e$  is required. Transient transport analysis shows the strong reduction of  $\chi_{tr} = (1 + \beta)\chi_e$  inside the ITB region (see Fig. 5 (c) and (d)). The small difference between  $\chi_{tr}$  and  $\chi_{pb}$  indicates  $\beta = 0$  (i.e. the ITB is in a “weak or not stiff” region). The growth of the cold pulse can be explained by the convective-like term driven by the  $T_e$  dependence of  $\chi_e$  (see Eq. 1) because the transient transport analysis indicates the negative  $T_e$  dependence of  $\chi_e$  ( $\chi_e$  decreases with an increase in  $T_e$ ). Figure 5 (e) and (f) show the  $T_e$  dependence factor  $\alpha$  of  $\chi_e$ . The negative  $T_e$  dependence ( $\alpha < 0$ ) is observed inside the ITB in LHD, while it is observed not only inside the ITB but also outside the ITB in JT-60U. The transport just outside the ITB region in JT-60U, where the flat  $T_e$  and  $q$  profiles are observed, may be different qualitatively from the transport shown in Fig. 3. Although the physical mechanisms that could be responsible for this negative  $T_e$  dependence of  $\chi_e$  are unclear yet (any gyro-Bohm models can not provide  $\alpha < 0$ ), the negative  $T_e$  dependence can contribute to the ITB formation. Effects of collisional zonal flow damping on turbulent plasma is one of the candidates to explain the negative  $T_e$  dependence of  $\chi_e$  [12]. The  $q$  profile effect may be a key issue that should be clarified because both plasmas in Fig. 5 have the negative magnetic shear configuration.

#### 4. Non-local effects in transport

Several recent experiments in LHD and JT-60U, however, point to the importance of non-local effects in the turbulent-induced transport [13]. Rapid cold pulse propagations are observed both in LHD and JT-60U. The typical time evolution of core temperature response to the edge cooling in JT-60U high- $\beta_p$  ELMy H-mode plasma ( $P_{NB} = 18\text{MW}$ ,  $R_{ax} = 3.3\text{m}$ ,  $a_p = 0.93\text{m}$ ,  $\bar{n}_e = 3 \times 10^{19}\text{m}^{-3}$ ,  $I_p = 1.8\text{MA}$ ) is shown in Fig. 6(a). The core  $T_e$  begin to decrease before diffusive transport effect (calculated by  $\chi_{pb}$ ) reaches this region, and the magnitude of cold pulse is larger than that predicted by diffusion. The transient analysis with an empirical non-linear  $\chi_e$  model indicates the strong  $\nabla T_e$  dependence of  $\chi_e$  ( $\beta = 9$ ). This large  $\beta$  is not consistent with the

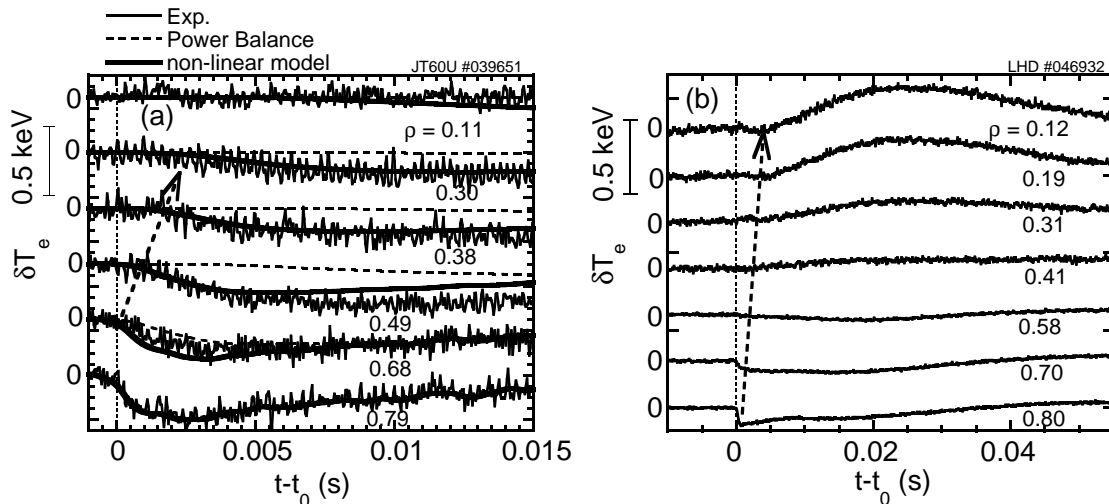


FIG. 6: Time evolution of  $T_e$  perturbations at different radii in (a) JT-60U high- $\beta_p$  ELMy H-mode plasma and (b) LHD ECH + NBI plasma. The simulation results with the linear  $\chi_e$  model ( $\chi_e = \chi_e$  i.e.  $\alpha = 0, \beta = 0$  in the non-linear model) and the non-linear  $\chi_e$  model ( $\alpha = 0, \beta = 9$ ) are also shown in (a). The TESPEL is injected at  $t = t_0$ .

power degradation observed in JT-60U. One of the non-linear but local models (e.g. ITG-based models [14]) can explain such a large  $\beta$ , however, there is no evidence of rapid changes in the fluctuations or  $T_i$  profile.

It has been observed that the non-local response to edge cold pulses often have reversed polarity, with the core  $T_e$  increasing in response to edge cooling in many tokamaks [15, 16]. While such a phenomenon, which can not be explained by the local diffusive model even if the heat flux is a non-linear function of  $\nabla T_e$  and  $T_e$ , has not been reported so far in helical systems. However, a first observation of the reverse of  $\delta T_e$  polarity in helical systems is done in LHD, and thus the strong non-local effects in helical systems is evident as well as in tokamaks. The typical  $T_e$  response to the edge cooling in LHD is shown in Fig. 6(b). The TESPEL is injected to the edge of plasma ( $P_{EC} \sim 0.8\text{MW}$ ,  $P_{NB} \sim 2\text{MW}$ ,  $T_{e0} = 3\text{keV}$ ,  $\bar{n}_e = 1 \times 10^{19}\text{m}^{-3}$ , same magnetic configuration as Fig. 2). The cold pulse produced in the edge region ( $\rho > 0.8$ ) is strongly reduced in the region of  $0.4 < \rho < 0.6$ , and thus neither  $T_e$  nor  $\nabla T_e$  are changed significantly by the cold pulse propagation. In spite of no change in temperature and its gradient, a sudden rise of  $T_e$  is observed in the central region ( $\rho < 0.4$ ). This indicates an abrupt reduction of  $\chi_e$  unrelated to  $\nabla T_e$  and/or  $T_e$ . Unfortunately, plasma goes back to normal condition after 20ms from TESPEL injection as well as in tokamaks. There are some discoveries in the characteristics of the non-local  $T_e$  rise observed in LHD, (1) The non-local  $T_e$  rise is also observed in plasmas sustained by pure ECH, (2) The formation of e-ITB is triggered by a non-local  $T_e$  rise in LHD when the plasma is heated by just below the critical power, (3) The non-local  $T_e$  rise is also observed in the e-ITB plasma. These new observations will help to make a physical picture of the turbulence, which can explain both non-linearity and non-locality in transport. Especially, observation (1) indicates the plasma current itself is irrelevant to the non-local transport mechanism. Moreover, the similarities of the non-local  $T_e$  rise between tokamaks and LHD allow us to conclude that the magnetic shear is not important in the non-local transport. The non-local  $T_e$  rise in LHD is unclear in the high- $n_e$  and low- $T_e$  region ( $n_e > 1.5 \times 10^{19}\text{m}^{-3}$ ,  $T_e < 2.0\text{keV}$ ) just as TFTR scaling predicts [16]. The non-local  $T_e$  rise, however, has not been observed in JT-60U even if

$n_e$  and  $T_e$  are in condition, which is predicted by TFTR scaling.

## 5. Summary

Cold/Heat pulse propagation experiments in LHD and JT-60U show the following electron heat transport features. (i) Cold pulses in no-ITB plasma in LHD ( $\nu_* = 0.1 - 0.3, \rho_* = 3 - 4 \times 10^{-3}$ ) show a gyro-Bohm like  $T_e$  dependence of  $\chi_e$ . On the other hand, heat pulse propagations show not only the gyro-Bohm like  $T_e$  dependence of  $\chi_e$  but also the  $\nabla T_e$  dependence of  $\chi_e$  in the core region ( $\rho < 0.3$ ) of JT-60U plasma ( $\nu_* = 0.01 - 0.1, \rho_* = 4 - 10 \times 10^{-3}$ ). (ii) The negative  $T_e$  dependence of  $\chi_e$  is found in LHD and JT-60U plasmas with reversed magnetic shear and e-ITB. (iii) The prompt cold pulse propagation in a high- $\beta_p$  ELMy H-mode plasma in JT-60U and the reverse of cold pulse polarity in low density plasmas ( $n_e < 1 - 1.5 \times 10^{19} \text{m}^{-3}$ ) are evidence for non-local heat transport.

## Acknowledgments

This work was carried out as a joint work under the Facility Utilization Program of JAERI.

## References

- [1] F. Wagner *et al* , Phys. Rev. Lett. **56** (1986) 2187
- [2] J. D. Callen *et al* , Phys. Fluids B **4** (1992) 2142
- [3] H. Yamada *et al* , Nucl. Fusion **43** (2003) 749
- [4] W. Horton *et al* , Phys. Fluids **31** (1988) 2971
- [5] F. Romanelli and S. Briguglio, Phys. Fluids **B 2** (1990) 754
- [6] F. Ryter *et al* , Phys. Rev. Lett. **86** (2001) 5498
- [7] N. J. Lopes Cardozo, Plasma Phys. Control. Fusion **37** (1995) 799
- [8] S. Sudo *et al* , Plasma Phys. Control. Fusion **44** (2002) 129
- [9] K. Tanaka, this conference
- [10] R. Waltz and A. Boozer, Phys. Fluids B **5** (1993) 2201
- [11] T. Fujita, Phys. Rev. Lett. **78** (1997) 2377
- [12] Z. Lin *et al* , Phys. Rev. Lett. **83** (1999) 3645
- [13] S. V. Neudatchin, Plasma Phys. Control. Fusion **44** (2002) A383
- [14] M. Kotschenreuther *et al* , Phys. Plasmas **2** (1995) 2381
- [15] K. W. Gentle *et al* , Phys. Rev. Lett. **74** (1995) 3620
- [16] M. W. Kissik *et al* , Nucl. Fusion **38** (1998) 821